Scientific Reports

https://doi.org/10.1038/s41598-026-45923-1

Article in Press

Evaluating miscible gas injection patterns for enhanced oil recovery in fault controlled fractured vuggy volatile oil reservoirs

Received: 11 March 2025

Accepted: 23 March 2026

Published online: 03 April 2026

Cite this article as: Deng X., Liu Z., Zhang J. *et al.* Evaluating miscible gas injection patterns for enhanced oil recovery in fault controlled fractured vuggy volatile oil reservoirs. *Sci Rep* (2026). https://doi.org/10.1038/s41598-026-45923-1

Xingliang Deng, Zhiliang Liu, Jie Zhang, Zhouhua Wang, Guohui Li, Hanmin Tu, Peng Wang & Chao Zhang

Evaluating Miscible Gas Injection Patterns for Enhanced Oil Recovery in Fault Controlled Fractured Vuggy Volatile Oil Reservoirs

Xingliang Deng[a, b, d], Zhiliang Liu[a, b, c], Jie Zhang[a, b], **Zhouhua Wang**[e*], Guohui Li[a], Hanmin Tu[e], Peng Wang[a, b], Chao Zhang[a]

[a]*PetroChina Tarim Oilfield Company, Korla, Xinjiang, China;*

[b]*R&D Center for Ultra Deep Complex Reservoir Exploration and Development, CNPC, Korla, China;*

[c]*Xinjiang Key Laboratory of Ultra-deep Oil and Gas, Korla, Xinjiang, China;*

[d]*State Energy Key Laboratory for Carbonate Oil and Gas, Korla, Xinjiang, China;*

[e]*State Key Laboratory of Oil and Gas Reservoir Geology and Exploitation, Southwest Petroleum University, Chengdu, China.*

****

Corresponding author:

Prof. Zhouhua Wang

Email: wangzhouhua@126.com

State Key Laboratory of Oil and Gas Reservoir Geology and Exploitation, Southwest Petroleum University, Chengdu, 610500, China.

****

Evaluating Miscible Gas Injection Patterns for Enhanced Oil Recovery in Fault Controlled Fractured Vuggy Volatile Oil Reservoirs

ABSTRACT: The FM fault-controlled fractured-vuggy volatile oil reservoir is characterized by strong heterogeneity and insufficient natural energy, which limits the effectiveness of conventional water flooding due to early water breakthrough and significant attic oil retention. To optimize post-waterflood development strategies, this study conducted a series of full-diameter physical simulation experiments using multi-fractured-vuggy cores under reservoir conditions. Experiments with different gas injection media revealed that the stage recovery rates for N_2, hydrocarbon gases, and CO_2 are 78.85%, 64.36%, and 59.96%, with an identical gas injection volume of 0.77 HCPV. Based on these findings, along with the results from phase behavior experiments, N_2 is recommended as the preferred gas injection medium. The cumulative oil recovery after continuous water flooding was about 75%. The subsequent water-alternating-gas (WAG) injection effectively increased oil recovery by approximately 6.6-8.8% relative to waterflooding alone by improving sweep efficiency and mobilizing residual oil in branch fractures. Finally, connectivity-controlled case studies demonstrate that gas injection in upper-connected fractured-vuggy unit provides an additional 11.68% incremental recovery compared with lower-connected unit due to delayed gas breakthrough and expanded sweep volume. Overall, direct

continuous gas injection results in earlier gas breakthroughs, premature oil production at the core outlet, reduced gas consumption per ton of oil, and favorable extraction outcomes. Therefore, it is recommended to implement a direct continuous gas injection in the well group following water flooding to enhance crude oil recovery.

Keywords: Fault-controlled fracture-vuggy volatile reservoirs, gas injection flooding, miscible flooding, enhanced oil recovery, physical simulation

1 Introduction

The FM oilfield, classified as a fault-controlled fracture-cave volatile oil reservoir, is distinguished by its slab-like features along faults. Currently, the natural energy of the reservoir experiences a rapid decline following crude oil degassing, which necessitates urgent energy supplementation. Despite extensive water injection research and field practices, several challenges persist. These challenges include rapid water channeling in specific wells and high residual oil concentrations in the upper sections during the later stages of water injection. Initial successes in gas injection recovery have simulated further investigation into the viability of gas injection to enhance oil recovery.

In the gas injection process for oil recovery, the selection of an appropriate gas injection medium is critical to enhance the effectiveness of the recovery process. Carbon dioxide (CO_2) is the most commonly used gas, while CH_4, N_2, and other hydrocarbon gases also present significant potential[1-4]. Hu et al. [5] conducted experiments on crude oil properties, phase behavior, and numerical simulations to compare the mechanisms and effects of N_2 and CO_2 injections in the fracture-cave carbonate reservoirs of the Tahe oilfield. Their findings indicated that non-miscible N_2 injection was more effective than

miscible CO_2 injection. Heidari et al. [6] performed both miscible and non-miscible gas injection experiments on fractured carbonate rocks, assessing the efficiency of CO_2, N_2, and CH_4 for oil recovery, and concluded that CO_2 was the most effective. Notably, when reservoir pressure significantly exceeds the miscible pressure of the gas, CO_2 increases the density of crude oil, which impairs gravity drainage efficiency and subsequently reduces the recovery rate. Mohsenzadeh et al. [7] investigated the effects of three different gases (pure CO_2, pure N_2, and a mixture of 15% CO_2 and 85% N_2) on crude oil recovery in carbonate reservoirs under reservoir conditions using a fractured reservoir physical model. Their results demonstrated that piston-like displacement achieved by N_2 injection resulted in the highest oil recovery rate within the fractures, while CO_2 injection formed stable foam oil in the fractures, which trapped more oil and hindered heavy oil recovery prior to gas breakthrough.

Due to the differing densities of oil and water, fracture-cave reservoirs often retain a substantial amount of attic oil following water injection. Non-miscible gas injection generally leads to the formation of a secondary gas cap, while gravity drainage effectively reduces the oil column height, facilitating the displacement of attic oil that accumulates in the upper sections post-water injection [8-14]. Wu et

al. [15] developed a visual, physical model of the fracture-cave carbonate reservoir in the Tahe oilfield and conducted simulation experiments involving water and gas injection. Their findings revealed that when strong bottom water interacts with injected gas, a slug-like water-gas interval is formed, which reduces gas phase permeability and inhibits gas channeling. Thus, it helps in recovering residual oil after water injection.

Similarly, Kang et al. [16] utilized actual cores from the fracture-cave reservoirs in the Tarim Basin, performing artificial fracture and cavity treatments along with physical simulation experiments. They concluded that gas injection is more effective under conditions of good reservoir connectivity, minimal and well-connected bottom water, and high reservoir pressure recovery during gas injection. Furthermore, Shi et al. [17] addressed the high water cut issue prevalent in the later stages of fracture-cave reservoirs by developing a fracture-cave model and conducting gas injection displacement experiments. The results indicated that residual oil remains in the model after water flooding, and the injection of N_2 could enhance fluid flow and improve recovery.

Experimental research and field trials indicate that the effectiveness of gas injection for oil recovery is influenced by both the type of gas injected and the method of injection employed. Hui et al.

[18] developed a two-dimensional visual displacement model specifically for fracture-cave reservoirs and conducted experiments on water injection, gas injection, and Water Alternating Gas (WAG) injection. The results indicated that, due to the differing densities of oil, gas, and water, water injection effectively displaced residual oil at the bottom of the reservoir, while gas injection resulted in the formation of a secondary gas cap that displaced residual oil in the upper sections. WAG injection achieved the most favorable results, yielding optimal crude oil recovery. Additionally, Allal et al. [19] conducted a WAG injection test in the "R" oilfield, finding that controlling mobility and front displacement through water injection significantly enhanced the efficiency of miscible gas injection. The separation of the injected fluids created unswept areas, making it easier to control the gas-oil ratio, water breakthrough trend, and maintain reservoir pressure. Shedid et al. [20] performed continuous CO_2 injection and WAG injection experiments on severely heterogeneous carbonate reservoir cores. They found that WAG injection was more effective, with an optimal slug size of 0.15 HCPV. Hou et al. [21] used a two-dimensional visual profile model of fracture-cave reservoirs to investigate the effects of nitrogen injection rate, timing, and method on recovery efficiency when bottom water energy

is insufficient. The results indicated that both excessively high and low gas injection rates resulted in reduced final recovery efficiency, while the timing of gas injection influenced recovery efficiency by affecting the effectiveness of water flooding. WAG injection was found to be significantly more effective than continuous gas injection.

Factors such as fractures, cavities, and injection positions all affect the effectiveness of the gas injection, necessitating tailored physical simulation experiments that consider the specific characteristics of the reservoir. The key to simulating fracture-cave carbonate reservoirs lies in obtaining cores that accurately represent fractures and cavities under reservoir conditions. Currently, two primary methods are used for physical simulation: one utilizes etched transparent glass plates to simulate the reservoir, while the other incorporates actual reservoir cores with artificially created fractures and cavities [22]. Although transparent glass plate models effectively capture the flow patterns of oil and gas, as well as the dynamics of reservoir exploitation, their limited pressure-bearing capacity poses challenges in simulating the actual conditions of most oil and gas reservoirs [23-26]. Li Jun et al. [27] utilized seismic data from the Tahe oilfield and outcrop cores to create artificial fractures and cavities. They designed network fracture-cave models and series fracture-cave

models. However, achieving reliable matching patterns and accurate reserve distribution using this core carving method presents challenges[28], as it does not fully align with the characteristics of fault-controlled fracture-cave reservoirs. Additionally, the development of fracture-cave models must take into account factors such as the shapes of cavities and the distribution of both fractures and cavities.

The FM oilfield faces significant challenges due to its inadequate natural energy resources, which result in a limited stable production period during the water injection development. Initial field tests of gas injection have indicated a potential for enhanced oil production. However, the specific types of gas, injection techniques, and underlying mechanisms are not yet well understood. This paper addresses these reservoirs by employing a numerical reservoir profile to analyze and extract the shapes and distributions of storage spaces within the reservoir core. It prepares representative fault-controlled fracture-cave cores that accurately match the proportions of pores, fractures, and cavities observed in the reservoir. Through physical simulation experiments on gas injection in volatile fault-controlled fracture-cave reservoirs, this study aims to optimize the gas injection medium, methodology, timing, and connectivity locations. These

findings provide a theoretical foundation for advancing gas injection development in the FM oilfield.

2 Experiment Methods

2.1 Fluid sample

The crude oil used in this experiment was prepared in accordance with the original PVT report from well M1. The prepared crude oil exhibited a gas-oil ratio (GOR) of 502 m^3/m^3, a bubble point pressure of 36.36 MPa, a density of 0.5013 g/cm^3, and a viscosity of 0.411 mPa·s. A detailed composition of the prepared crude oil is provided in Table 1.

Table 1. Composition of the crude oil.

Component	N_2	CO_2	C_1	C_2	C_3	iC_4
mol%	1.57	2.51	63.16	5.02	3.38	1.11
Component	nC_4	iC_5	nC_5	C_6	C_7	C_8+
mol%	2.46	1.27	1.83	4.72	2.83	10.15

The gases used for injection in the experiment included N_2, hydrocarbon gas, and CO_2. Both N_2 and CO_2 were commercial gases with a purity of 99.95%, whereas the hydrocarbon gas was laboratory-prepared. This hydrocarbon gas was rich in C_1, containing 81%, as detailed in Table 2.

Table 2. Composition of injected hydrocarbon gas.

Component	N_2	CO_2	C_1	C_2	C_3	iC_4
mol%	4.61	1.58	81.02	8.07	3.43	0.46
component	nC_4	iC_5	nC_5	C_6	C_7	

mol%	0.64	0.08	0.07	0.03	0.01	

The total salinity of the prepared formation water is 2,498,000 mg/L, and it is classified as $CaCl_2$ type. Detailed water quality information is presented in Table 3.

Table 3. Formation water ion content.

Positive ion	K^++Na^+	Ca^{2+}	Mg^{2+}	Ba^{2+}
Content (mg/L)	74504	18200	1630	18.26
Negative ion	Cl^-	HCO_3^-		SO_4^{2-}
Content (mg/L)	1540000	3.24		3494

2.2 Core sample

Fracture-controlled vuggy volatile oil reservoirs exhibit strong heterogeneity, which complicates the acquisition of representative core samples. In this study, representative cores were prepared using a method known as vug carving. Outcrop cores that closely matched the reservoir's lithology, diagenesis, pore structure, and fracture characteristics were selected for this purpose. Reservoir fracture-vuggy geometry was digitized from a digital profile of the reservoir schematic (Figure 1) and translated into CNC machining parameters to replicate natural pore-vug-fracture proportions.The carved core measured 10 cm in diameter and 15 cm in length, with the parameters for the fracture carving as shown in Table 4.

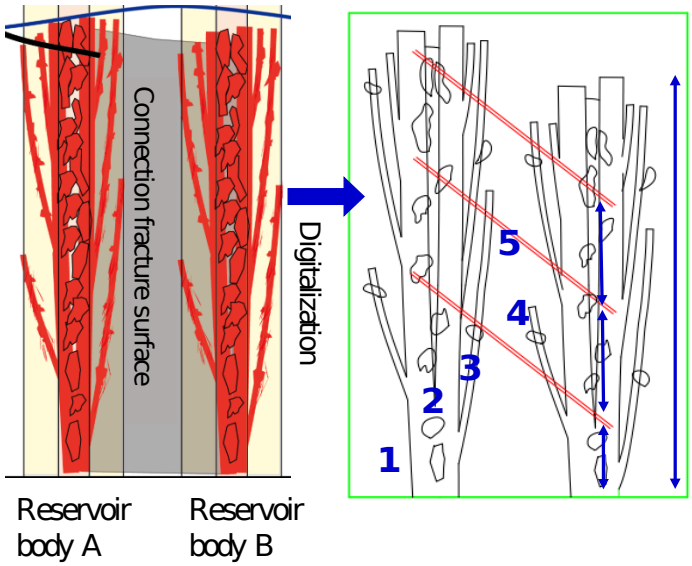

Figure 1. Schematic diagram of core sample: 1. reservoir body A; 2. main fracture; 3. branch fracture; 4 reservoir body B; 5. communicating fracture (65°).

Table 4. Fracture carving parameters.

Fracture type	Main fracture	Branch fracture	Communicating fracture
Width (mm)	8	2	1
Depth (mm)	20	20	20

In the experiment, copper oxide was employed to seal the communicating fractures within the cores to compare the effects of various connection positions on gas injection for oil displacement. The different connectivity conditions of the cores are illustrated in Figure 2.

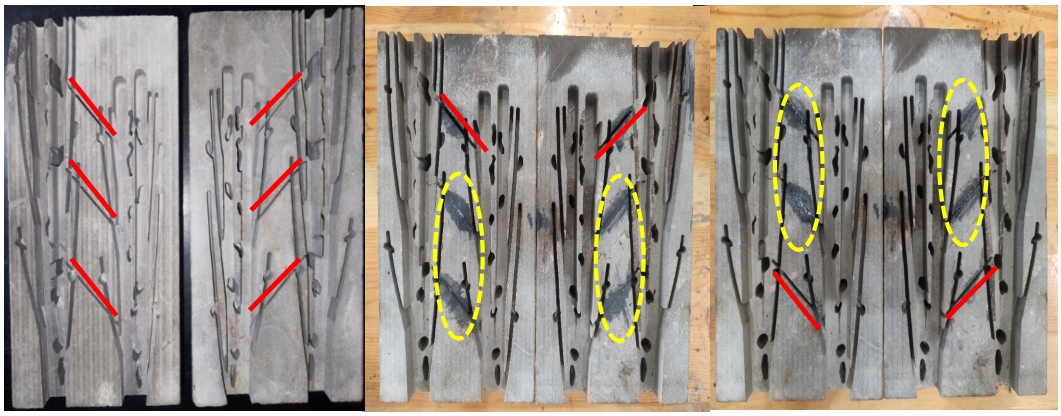

(a) (b) (c)

Figure 2. Core sample with different connectivity conditions: (a) fully connection; (b) upper connection; (c) lower connection.

To simulate pore collapse, rock fragments sized 10-14 mesh and 16-20 mesh were combined in a 1:1 mass ratio to fill the carved cores, illustrated in Figure 3. After filling, the core exhibited a permeability of 51.8 mD and a porosity of 5.76%. These parameters were measured to ensure that the experimental setup closely matched the reservoir.

Figure 3. Typical fault control fracture cavity filling rock core.

2.3 Experiment setup

The physical simulation experiment for gas injection oil displacement in fracture-controlled vuggy volatile oil reservoirs is depicted in Figure 4.

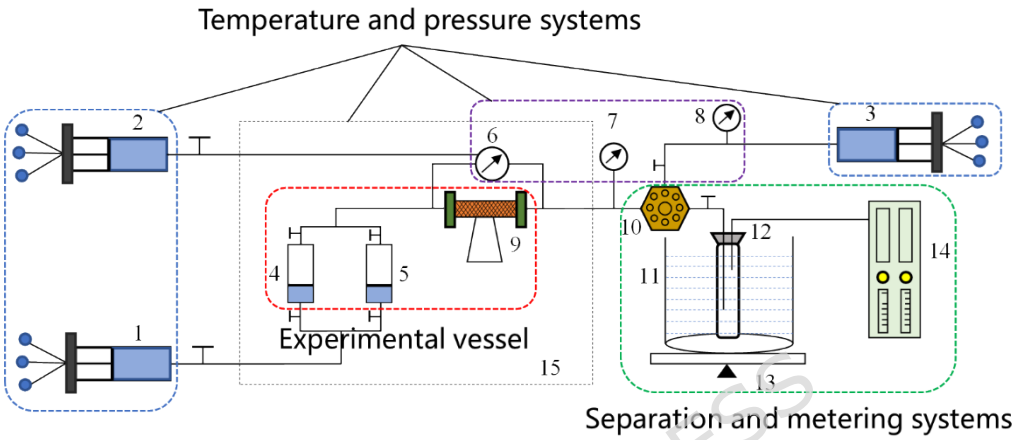

Figure 4. Flow chart of gas injection and oil recovery experiment: 1. displacement pump; 2. confining pressure pump; 3. back pressure pump; 4 and 5. intermediate container; 6, 7 and 8. pressure gauges; 9. core holder; 10. back-pressure valve; 11. condensation device; 12. gas-liquid separator; 13. electronic balance; 14. gas meter; 15. oven.

2.4 Experimental plan and steps

Prior to the gas injection displacement experiments, preliminary tests were performed, which included gas injection expansion and minimum miscible pressure (MMP) experiments. These preliminary tests analyzed the phase behavior of crude oil with different gases (N_2, hydrocarbon gases, CO_2). The gas injection expansion tests were conducted following the Chinese standard "GB/T 26981-2020", while

the MMP tests adhered to the Chinese standard "SY/T 6573-2016" method.

The experimental design for gas injection optimization is presented in Table 5, which outlines nine distinct experimental setups. The experiments were performed above the bubble pressure. Schemes 1, 2, and 3 concentrated on continuous gas injection utilizing N_2, hydrocarbon gases, and CO_2 to determine the optimal gas medium. Schemes 4, 5, 6, and 7 employed the identified optimal gas medium for post-water flooding gas injection experiments, investigating various injection methods (Schemes 4, 5, 6) as well as the timing of gas injection (Schemes 5, 7). Finally, Schemes 8 and 9 explored the influence of different core connection positions on oil displacement efficiency.

Table 5. Design of optimal experimental plan for gas injection.

<table>
<tr><th rowspan="2">Case</th><th rowspan="2">Core connectivity method</th><th rowspan="2">Water injection stage</th><th colspan="3">Gas injection stage</th></tr>
<tr><th>Timing of gas injection</th><th>Gas injection medium</th><th>Gas injection method</th></tr>
<tr><td>1</td><td rowspan="4">Fully connected</td><td rowspan="3">/</td><td rowspan="3">1.2Pb (43.6MPa)</td><td>N_2</td><td rowspan="3">Continuous gas drive 1.5Pb (54MPa)</td></tr>
<tr><td>2</td><td>Hydrocarbon gas</td></tr>
<tr><td>3</td><td>CO_2</td></tr>
<tr><td>4</td><td>Bottom injection and top</td><td>Water drive finished</td><td>Optional selection medium</td><td>Continuous gas drive 1.65Pb(60MPa)</td></tr>
</table>

5		production 1.5Pb (54MPa)			Gas water alternate drive, water to gas ratio 1:1, 1.65Pb (60MPa)
6					Gas water alternate drive, water to gas ratio 1:2, 1.65Pb (60MPa)
7					Gas water alternate drive, water to gas ratio 1:1,1.8Pb (65.4MPa)
8	Upper connection	/	1.2Pb (43.6MPa)	Optional selection medium	Continuous gas drive, 1.5Pb (54MPa); Gas water alternate drive, water to gas ratio 1:1, 1.65Pb (60MPa)
9	Lower connection				

The steps for optimizing gas injection in experimental tests are outlined as follows:

(1) **Formation Conditions Establishment**: The experimental apparatus is assembled and heated to a temperature of 150.3°C. Degassed crude oil is then injected into the core, and the pressure is raised to 84.05 MPa. Following this, the degassed oil is displaced with the prepared formation crude oil. After the

complete replacement of the degassed oil, the initial conditions are successfully established. The initial fluid saturations were established at 100% oil saturation after the replacement of degassed crude oil.

(2) **Natural Energy Depletion Phase**: The back pressure is reduced to lower the outlet pressure. The back pressure is decreased in a reduction of 4 MPa and stabilized until there is no gas production from the outlet for 5 minutes. During this stage, both gas and oil outputs are recorded. This process continues until the outlet pressure reaches $1.2P_b$ (43.6 MPa).

(3) **Water Flooding Stage**: In experimental schemes 4 to 7, the top of the simulated reservoir is closed, while the bottom is left open. The water injection pressure is increased to $1.5P_b$ (54 MPa). Subsequently, the top is opened for production, and water is injected from the bottom at a rate of 0.125 ml/min until no oil is produced from the outlet.

(4) **Continuous Gas Injection/WAG Phase**: The upper section of the simulated reservoir is opened, and the gas injection pressure is increased to specified levels ($1.5P_b$, $1.65P_b$, $1.8P_b$). Gas injection or WAG experiments are performed from the top at a

rate of 0.125 ml/min, with production occurring from the bottom until no oil is produced from the outlet.

3 Results and Discussion

3.1 Gas injection expansion experiment

These experiments aim to investigate the impact of injection gases on the phase behavior of crude oil. The experiments were carried out by mixing these gases with crude oil in a high-pressure cell at a reservoir temperature of 150.3°C. As the mole percentage of gas increased, measurements were taken to assess changes in oil properties. Figure 5 illustrated that an increase in the volume of injected gas resulted in higher oil saturation pressure and formation volume factor, while oil viscosity and density exhibited a decrease.

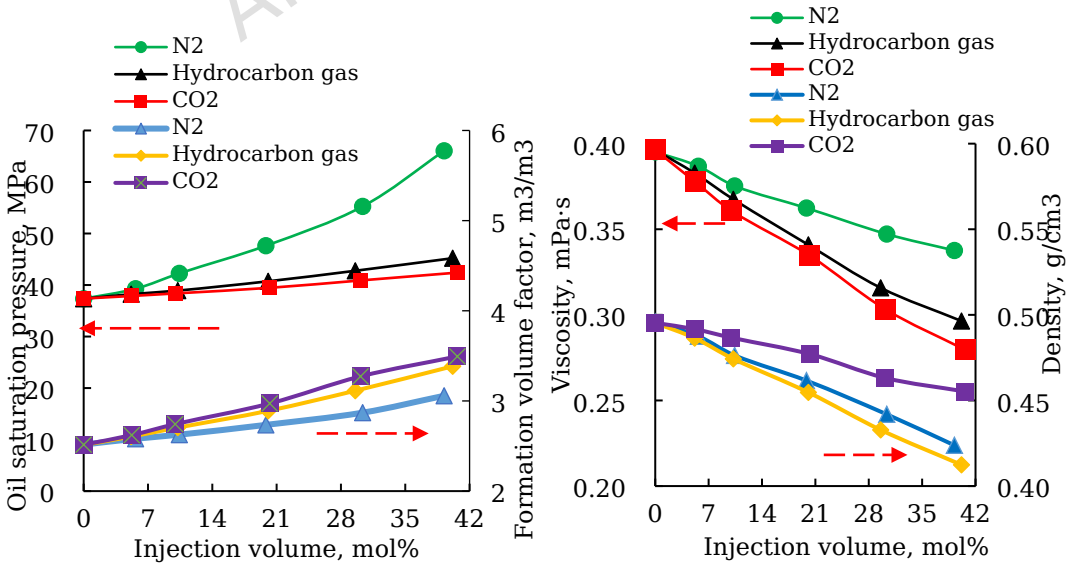

(a)

(b)

Figure 5. Changes in physical properties of crude oil: (a) changes in saturation pressure and volume coefficient of crude oil; (b) changes in viscosity and density of crude oil.

The experimental results indicate that nitrogen (N_2) exhibits significantly lower solubility in crude oil when compared to the other two gases. With a constant injection volume, carbon dioxide (CO_2) is identified as the most effective gas for reducing viscosity, whereas hydrocarbon gases are the most effective for decreasing density.

3.2 Slim-tube test

The slim tube experiments involved the injection of gases into crude oil samples at various pressures, aimed at measuring the oil displacement efficiency at a reservoir temperature of 150.3°C. The gases were injected to a maximum of 1.2 Pore Volume (PV) across different pressures. Figure 6 presents the results of oil displacement efficiency under these varying injection pressures. The MMPs for N_2, hydrocarbon gas, and CO_2 with crude oil were 42.19 MPa, 38.03 MPa, and 37.36 MPa, respectively. These findings suggest that CO_2 is the most effective for miscible displacement. For the volatile oil in well M1, all three gases can achieve miscibility with the formation of crude oil at a shut-in pressure of 43.6 MPa.

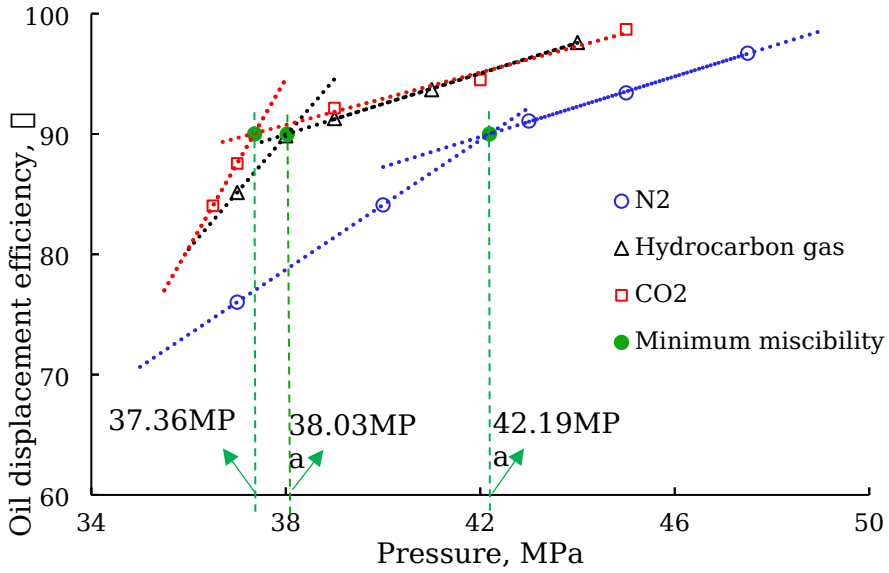

Figure 6. MMPs between different injected gases and crude oil.

3.3 Gas Injection Experiment

3.3.1 Gas Injection Media optimization

As the natural energy of fracture-controlled vuggy volatile oil reservoirs depletes to above the bubble point pressure, continuous gas injection experiments were conducted using various injection media according to cases 1, 2, and 3 outlined in Table 5. During the natural energy depletion stage, the cumulative oil recovery was comparable across the three experiments. In the continuous gas injection stage, gas breakthrough was observed at 0.77 HCPV for N_2, 0.88 HCPV for hydrocarbon gases, and 0.95 HCPV for CO_2, as illustrated in Figure 7. The cumulative oil recovery at the point of breakthrough was 78.85% for N_2 (case 1), 71.76% for hydrocarbon gases (case 2), and 66.62%

for CO_2 (case 3), with highest oil recovery for N_2 injection, as illustrated in Table 6.

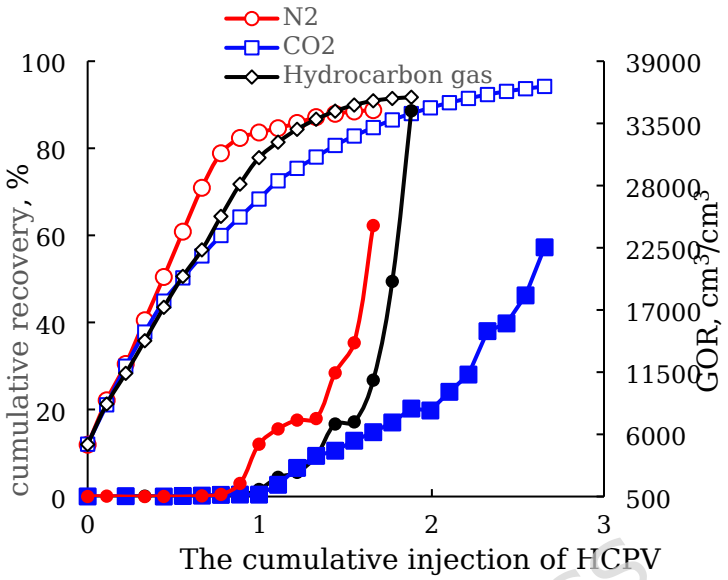

Figure 7. The cumulative recovery and GOR vary with the cumulative injection of HCPV.

Among the gases considered, N_2 exhibits the lowest solubility in crude oil. Consequently, N_2 injection gas breaks through the reservoir earlier and requires a smaller sweep volume. Due to gravitational segregation, N_2 easily forms a secondary gas cap within the core, effectively supplementing reservoir energy and enhancing the gravity drive effect. As a result, oil recovery rates with N_2 are superior compared to those achieved with hydrocarbon gases and CO_2. When the injected gas volume exceeds 1.0 HCPV, gas expansion experiments reveal that hydrocarbon gases and CO_2 have better solubility and miscibility with volatile oil than N_2. This disparity leads to a significant

reduction in viscosity, increased oil mobility, and larger gas sweep volumes, ultimately achieving a final oil recovery rate of over 90%.

Table 6. Oil displacement effects of different gas injection media.

Gas injection medium	N_2 (case 1)	Hydrocarbon gas (case 2)	CO_2 (case 3)
Recovery of oil during gas breakthrough(%)	78.85	71.76	66.62
The ultimate recovery rate of crude oil(%)	88.75	91.72	94.21
Gas consumption per ton of crude oil(m^3/t)	1803.05	2124.12	4058.97

While CO_2 injection yields the highest final oil recovery rate of 94.21%, it requires approximately twice the gas consumption per ton of oil compared to N_2 and hydrocarbon gases (see Table 6). In contrast, N_2 injection exhibits the lowest gas consumption per ton of oil and the shortest injection cycle. Moreover, N_2 injection achieves the highest oil recovery at gas breakthrough. Consequently, N_2 is identified as the optimal gas injection medium for FM fracture-controlled vuggy reservoirs.

3.3.2 Gas injection method optimization

In this study, experiment cases 4, 5, and 6 were conducted using the optimized medium N_2 to investigate the effects of gas injection. Prior to gas injection, water flooding was performed to simulate the water flooding process in fracture-controlled vuggy reservoirs. We

compared the oil displacement effects of continuous N_2 injection with those of N_2 WAG injection. During the natural energy depletion phase, the cumulative oil recovery across the three experiments was approximately 11.5% (see Figure 10). Cumulative oil recovery during continuous water flooding increased linearly until a water breakthrough occurred. Water injected from the bottom of the core displaced oil in a vertical piston-like manner, causing a uniform uplift of the oil-water contact and effective oil recovery. Following the water breakthrough, the water cut rapidly increased and stabilized at nearly 100% (Figure 8), which caused the oil production rate to diminish to almost zero. Ultimately, the cumulative oil recovery at the end of the water flooding was approximately 75%.

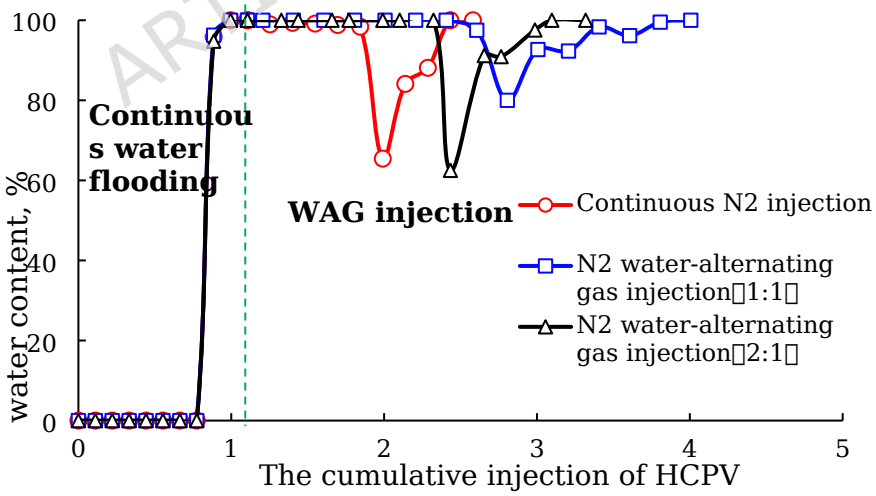

Figure 8. Changes in water content under different gas injection methods.

Following continuous water flooding, experiments were conducted to compare the effects of continuous gas injection with WAG injection on oil recovery. At this stage, water injection had been proven ineffective, with the water cut remaining approximately 100% both before and during the early stages of gas injection. Initially, gravity segregation between gas and water was pronounced. Gas injected from the top occupied the upper section of the reservoir, forming a secondary gas cap, while formation water descended along the primary fractures, resulting in a decline of the oil-water contact to decline (see Figure 9). Consequently, during the early stage, the water cut at the core outlet was elevated, yielding primarily formation water with negligible oil production. Once the oil-water contact reached the bottom of the production well, oil production began to increase. After the gas breakthrough, continued gas injection carried formation water that had accumulated at the reservoir's bottom due to gravity segregation. As the effectiveness of gas injection in displacing oil diminished, cumulative oil recovery decreased, and the water cut began to rise. Ultimately, as gas injection became less effective, the water cut returned to 100%.

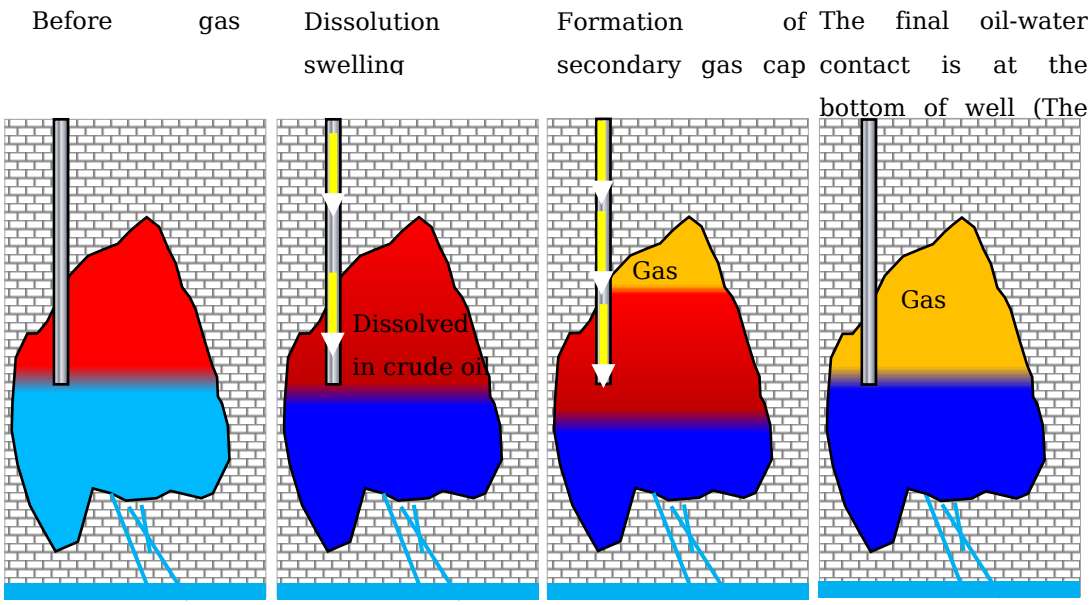

Figure 9. Schematic diagram of gas injection for oil recovery after water flooding.

Significant differences in oil displacement were observed during the gas injection stage. Figure 10 illustrates the GOR curves for continuous N_2 injection (case 4), WAG injection at a 1:1 ratio (case 5), and WAG injection at a 2:1 ratio (case 6). Prior to the gas breakthrough, the GOR remained stable at the initial level across all methods. However, it exhibited upward fluctuations post-breakthrough. Continuous N_2 injection resulted in the earliest gas breakthrough, with the GOR displaying smaller fluctuations while following an overall increasing trend. These fluctuations may be attributed to fluid supply from multiple fractures and vugs, which slightly reduced the GOR. In the WAG process, gas preferentially entered large pores during gas injection, displacing oil and raising the

GOR. Conversely, during water injection, the wetting and oil-washing effects of water displaced some oil from pores and throats, leading to a decrease in the GOR. Consequently, the GOR during WAG injection exhibited fluctuation, effectively enhancing oil mobility and increasing the swept volume.

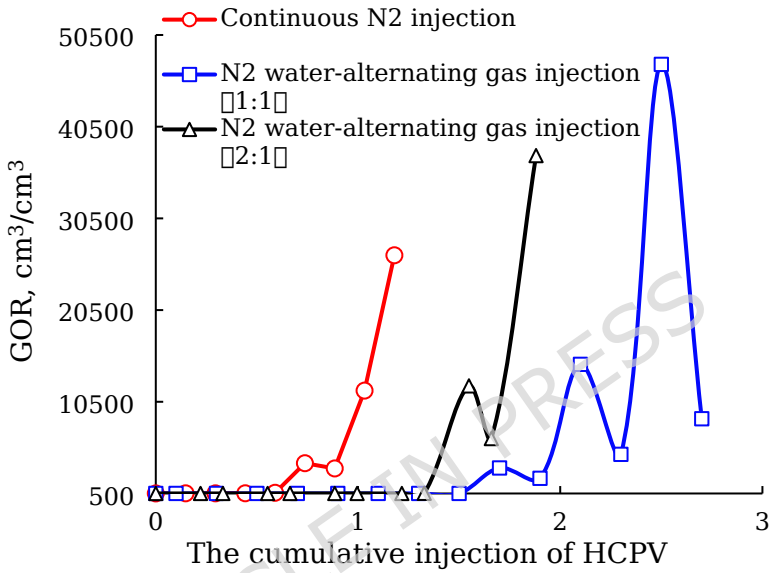

Figure 10. Changes in GOR under different gas injection methods during the gas drive stage.

Different gas injection methods yield varying recovery rates. Continuous gas injection achieves an incremental oil recovery rate of 5.8%, while WAG injection at ratios of 1:1 and 2:1 achieves incremental oil recoveries of 8.8% and 6.6%, respectively (see Figure 11). The g WAG injection enhances oil recovery by delaying gas channeling, and expanding the swept volume. The effectiveness of WAG injection is significantly influenced by the WAG ratio.

Specifically, a 1:1 ratio is more effective than a 2:1 ratio. However, continuous gas injection is characterized by earlier gas breakthroughs, earlier oil appearance at the core outlet, lower gas consumption per ton of oil, and effective recovery. Therefore, it is recommended to employ direct continuous gas injection following water flooding to enhance oil recovery.

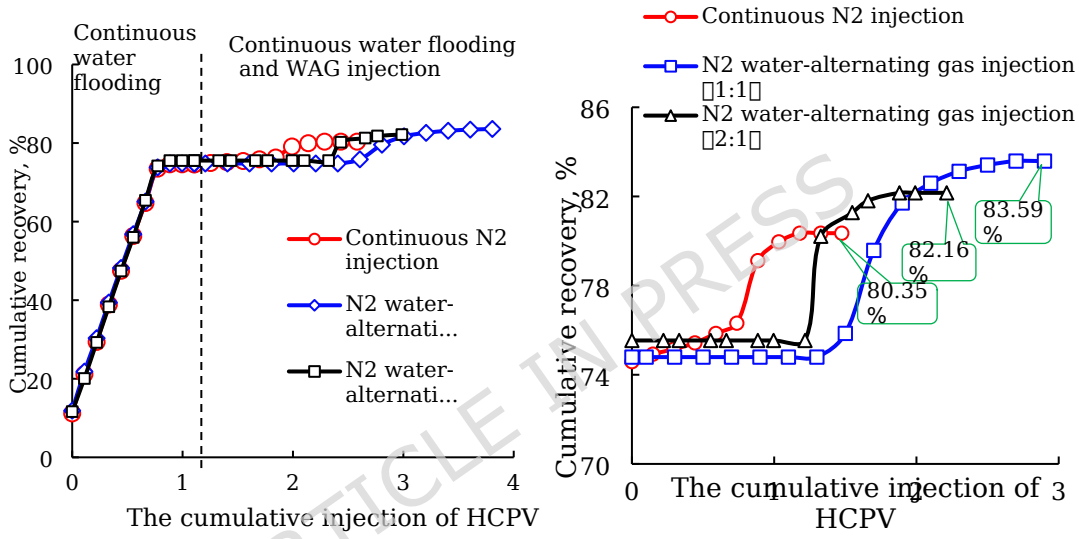

Figure 11. Comparison of crude oil recovery rates using different gas injection methods.

3.3.3 Gas injection timing optimization

Using the optimized medium N_2 in conjunction with formation water in a 1:1 WAG ratio for alternating injection as described in Scheme 7, we compared the experimental results with those obtained from Scheme 5. The depletion and water flooding stages produced consistent results under identical conditions, as presented in Table 7.

Table 7. Comparison of cumulative degrees of depletion and water drive stages.

Parameters	WAG after 1.65P_b (case 5)	WAG after 1.8P_b (case 7)
Depletion stage (%)	11.9	11.5
Water drive stage (%)	62.9	63.1
Ultimate recovery rate (%)	74.8	74.6

The results, presented in Figures 12 and 13, indicate that increasing the displacement pressure during WAG injection significantly enhances fluid flow velocity and diffusion within the reservoir. This improvement facilitates the gas's ability to penetrate fractures, vugs, pores, and low-permeability regions more effectively, thereby improving gas displacement capability, expanding the swept volume, enhancing oil displacement efficiency, significantly decreasing the water cut, and increasing the gas-oil ratio.

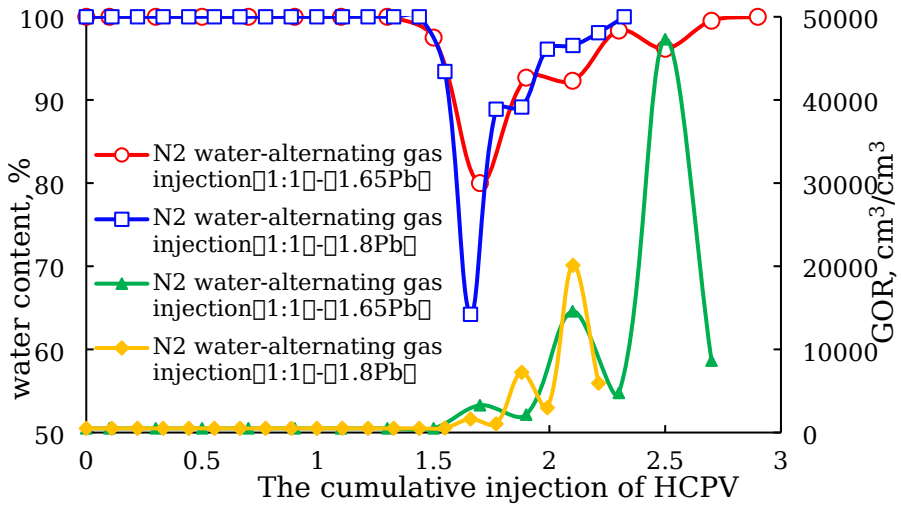

Figure12. Changes in water content and GOR in oil displacement at different gas injection timing.

Figure 13 illustrates that following the WAG stage, the incremental oil recovery at a displacement pressure of $1.8P_b$ reached 9.5%, which presents a 0.7% increase compared to that of $1.65P_b$. Research indicates that higher gas injection pressures improve oil displacement efficiency, while the overall difference in recovery between the two pressures remains minimal after the displacement stage. At the same injection volume, oil recovery at $1.8P_b$ outperforms that at $1.65P_b$. Elevated gas injection pressures facilitate increased gas injection, promote oil dissolution, improve oil mobility, and enhance displacement efficiency. Consequently, this leads to higher stage recovery, reducing the duration of the gas injection cycle.

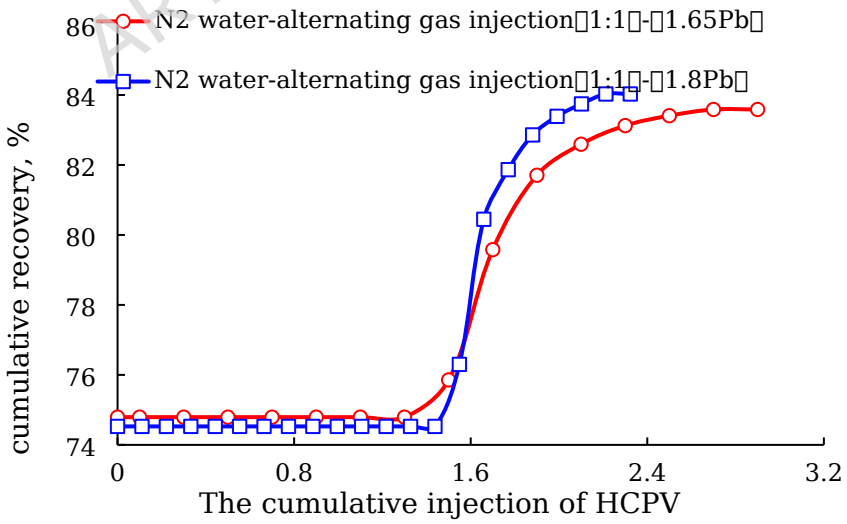

Figure 13. Comparison of crude oil recovery at different gas injection timing stages.

3.3.4 Optimal selection of connected positions

During the natural energy depletion stage, the oil recovery rates for fully connected, upper connected, and lower connected cores were approximately 11.5%. However, notable differences emerged during the N_2 continuous injection phase. The cumulative oil recovery was recorded at 77.34% for the fully connected core (case 1), 65.73% for the upper connected core (case 8), and 55.22% for the lower connected core (case 9). These results, which differ by over 10% (Figure 15), indicate that the position of connectivity significantly influences gas injection efficiency. Initially, gas injection produced a piston-like displacement, leading to comparable oil recovery rates across all models. However, when the injection volume reached 0.33 HCPV, the recovery curves began to diverge as gas entered connecting fractures. At this time, gas movement is illustrated by the green arrows in Figure 14. In the upper connected core, gas accessed the oil in both main fractures through the upper channel. In contrast, in the lower connected core, oil in the upper part of the left fracture was difficult to mobilize, as gas flowed along preferential paths, which reduced the swept volume and efficiency. Gas breakthrough occurred at 0.77 HCPV for the fully connected core, 0.66 HCPV for the upper connected core, and 0.55 HCPV for the lower connected core, as

presented in Figures 16. Following the breakthrough, mobilizing oil in lateral fractures became increasingly difficult, leading to a decline in the recovery rate. The fully connected core exhibited the latest breakthrough and the highest performance, whereas the lower connected core experienced the earliest breakthrough and the lowest recovery during the gas injection phase, which was attributed to its smallest swept volume.

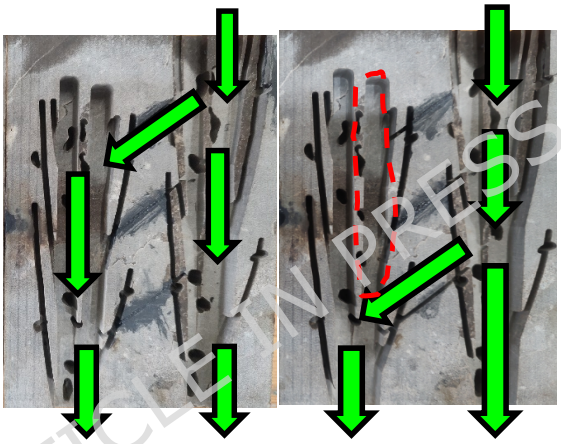

(a) (b)

Figure 14. Core at different connected positions: (a) upper connection sample; (b) lower connection sample.

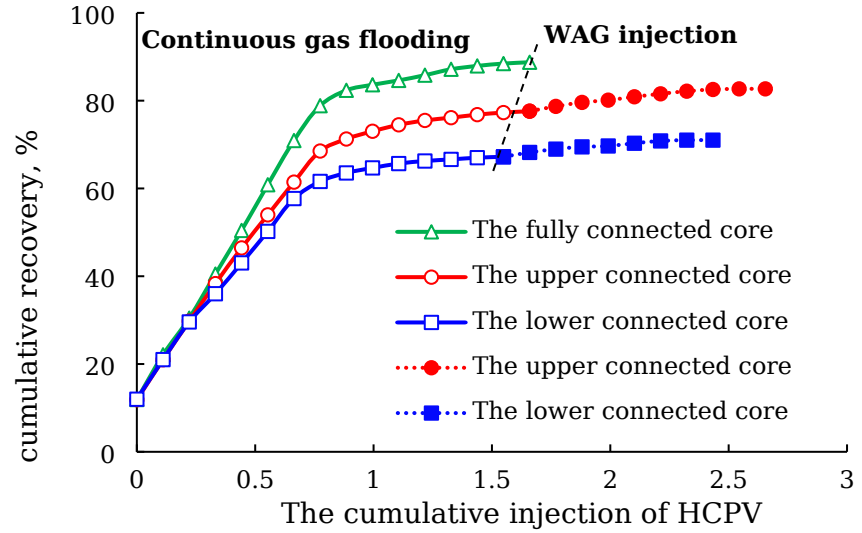

Figure 15. Comparison of cumulative recovery of crude oil in different oil recovery stages.

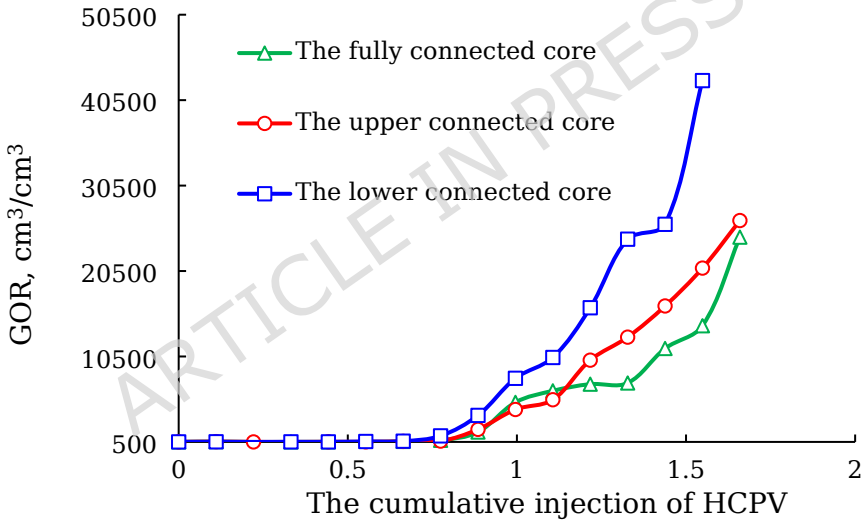

Figure 16. Comparison of changes in gas-oil ratio during pure N_2 flooding stage.

Following the failure of the N_2 drive, WAG injection was continued. Initially, the water cut was 0% as the injected gas effectively displaced the oil. However, when the cumulative WAG injection reached 0.22 HCPV, the water cut increased sharply to over

80%. As the injection process progressed, water began to penetrate smaller pores and throats, further displacing the residual oil. Nevertheless, the rate of increase in water cut subsequently began to decelerate due to the expanded swept area and enhanced efficiency in previously swept pores (Figure 17). During the WAG injection stage, the cumulative oil recovery was 5.1% for the upper connected core and 3.8% for the lower connected core. These findings suggest that transitioning to a WAG can further enhance the swept volume and facilitate the displacement of additional formation oil.

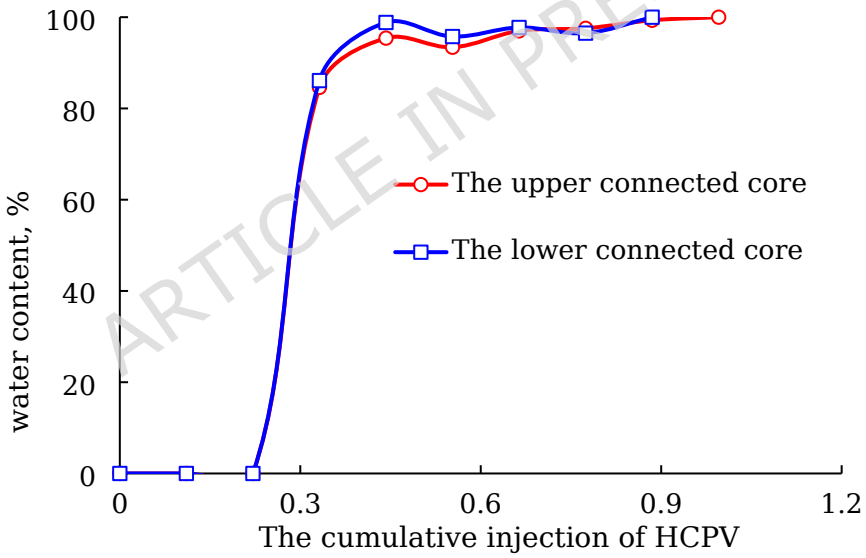

Figure 17. Comparison of water content during WAG stage.

Tables 8 and 9 present a comparative analysis of the depletion-gas injection and depletion-water flooding-gas injection methods applied to multi-fracture, multi-well units. From both an economic and

oil recovery perspective, the most effective approach for multi-well units is depletion followed by top N_2 gas injection.

Table 8. Comparison of different injection development methods.

Case	Depletion stage recovery rate of crude oil (%)	Gas drive stage recovery rate of crude oil when injection 1HCPV (%)	Accumulated injection volume (HCPV)	Ultimate recovery (%)
1	11.91	71.71	1.66	88.75
2	11.97	65.87	1.88	91.72
3	12.03	56.31	2.66	94.21
8	11.87	73.03	2.66	82.69
9	11.98	64.68	2.43	71.01

Table 9. Comparison of development methods of multiple fractured caves and multiple well units depletion water drive gas injection.

Case	Depletion stage recovery of crude oil (%)	The continuous water drive stage increased recovery (%)	Gas drive stage accumulated injection HCPV (%)	Accumulated injection volume (HCPV)	Ultimate recovery (%)
4	11.18	63.40	5.37	1.44	80.35
5	11.88	62.91	0	2.90	83.59
6	11.64	63.90	0	2.21	82.16
7	11.46	63.07	0	2.32	84.03

4 Conclusion

Based on an analysis of the fracture-controlled vuggy reservoir profile

and the carved vug volume in the FM oilfield, representative multi-fracture-vuggy cores were developed. Physical simulation experiments on gas injection development were conducted to provide valuable insights for improving oil recovery in such reservoirs.

(1) The FM oil reservoir is characterized by insufficient natural energy. Gas injection is primarily used to enhance the elastic expansion of crude oil and to reduce its viscosity. As a result, the expansion coefficient increases to a range of 1.21 to 1.39, while viscosity decreases by 14.8% to 29.4% relative to the un-injected crude oil. Under an average shut-in pressure of 43.6 MPa in single wells within the FM oilfield, N_2, hydrocarbon gas, and CO_2 can all achieve miscibility with the formation's crude oil. The minimum miscibility pressures for these gases are 42.19 MPa, 38.03 MPa, and 37.36 MPa, respectively.

(2) Experiments with different gas injection media revealed that during the depletion to shut-in pressure, the solubility of N_2 in formation crude oil is significantly lower than that of hydrocarbon gases and CO_2. The effect of gravity override is pronounced. At an identical gas injection volume of 0.77 HCPV, the stage recovery rates for N_2, hydrocarbon gases, and CO_2 are 78.85%, 64.36%, and 59.96%, respectively. Based on these

findings, along with the results from phase behavior experiments, N_2 is recommended as the preferred gas injection medium.

(3) The implementation of WAG injection following water flooding has been shown to effectively mobilize oil within lateral branch fractures, enhance the swept volume, and improve recovery rates by 6.6 to 8.8 percentage points compared to water flooding alone. The maximum incremental oil recovery rate reaches 8.8 percentage points, with a recommended WAG ratio of 1:1.

(4) Connectivity-controlled case studies reveal that upper-connected fractured-vuggy unit achieves 11.68 percentage points higher incremental recovery than lower-connected unit.

Data availability

The datasets generated during and/or analysed during the current study are not publicly available due to confidentiality concerns but are available from the corresponding author on reasonable request.

Acknowledgments

Acknowledgements: We extend our gratitude to Hanmin Tu and Zhouhua Wang for their intelligent discussions and support.

Author contributions

Investigation: X.D., Z.L., J.Z. Methodology: Z.W., H.T. Project administration: X.D., Z.L., G.L. Supervision: X.D., Z.L., P.W. Writing–original draft: Z.L., H.T., J.Z., C.Z. Writing–review & editing: X.D., Z.W., Z.L. Funding: X.D., Z.L.

Funding

This work was supported by China National Petroleum Corporation Major Science and Technology Project: Research on the Scaled Reserve Increase and Production and Exploration and Development Technology of Marine Carbonate Oil and Gas (No.2023ZZ16); Research on the Efficient Development and Improved Recovery of Ultra-deep Fault-controlled Marine Carbonate Reservoirs (No.2023ZZ16YJ02).

Disclosure statement

No potential conflict of interest was reported by the author(s).

Reference

[1] Yao, J., Wang, C., Yang, Y. et al. The construction of carbonate digital rock with hybrid superposition method. J. Pet. Sci. Eng. 110, 263–267 (2013).

[2] Manrique, E. J., Muci, V. E. & Gurfinkel, M. E. EOR field experiences in carbonate reservoirs in the United States. SPE Res Eval & Eng 10, 667–686 (2007).

[3] Wu, Y. B., Hu, D. D., Chang, S. W. et al. Application status of CO_2 flooding in low permeability reservoir to enhance oil recovery. Xinjiang Oil & Gas 6, 36–54 (2010).

[4] Li, F. & Yang, Y. C. Study of carbon dioxide drive in Pu 1-1 well and pilot experiment result analysis of Sha 1 reservoir in Pucheng Oilfield. Offshore Oil 29, 56–60 (2009).

[5] Hu, R. R., Yao, J., Sun, Z. X. et al. Study on EOR mechanism by gas injection replacing oil in fractured-vuggy carbonate reservoir of Tahe Oilfield. J. Xi'an Shiyou Univ. (Nat. Sci. Ed.) 30, 49–59 (2015).

[6] Heidari, P. & Kordestany, A. Gas injection into fractured reservoirs above bubble point pressure. Petrol. Sci. Technol. 30, 534–543 (2012).

[7] Mohsenzadeh, A., Escrochi, M., Afraz, M. et al. Non-hydrocarbon gas injection followed by steam–gas co-injection for heavy oil recovery enhancement from fractured carbonate reservoirs. J. Pet. Sci. Eng. 144, 121–130 (2016).

[8] Lyu, X. R., Liu, Z. C., Hou, R. J. et al. Mechanism and influencing factors of EOR by N2 injection in fractured-vuggy carbonate reservoirs. J. Nat. Gas Sci. Eng. 40, 226–235 (2017).

[9] Guo, W. J., Fu, S. S., Li, A. F. et al. Experimental research on the mechanisms of improving water flooding in fractured-vuggy reservoirs. J. Pet. Sci. Eng. 213, 110383; 10.1016/j.petrol.2022.110383 (2016).

[10] Lyu, X. R., Lyu, T., Xiao, F. Y. et al. Technical policy study of single well N_2 injection for EOR in complex fractured-vuggy carbonate reservoirs. J. Southwest Petrol. Univ. (Sci. Technol. Ed.) 43, 101–109 (2021).

[11] Parvizi, R. & Ghaseminejad, E. An experimental investigation of gravity drainage during immiscible gas injection in carbonate rocks under reservoir conditions. J. Petrol. Sci. Technol. 4, 63–71 (2014).

[12] Shi, F. G., Zheng, J. L., Qiao, Y. J. et al. Experimental study on oil flooding by full diameter core gas injection in fractured-vuggy reservoir. Adv. Fine Petrochem. 17, 9–11 (2016).

[13] Olabode, O. A., Orodu, O. D., Isehunwa, S. O. et al. Effect of foam and WAG (water alternating gas) injection on performance of thin oil rim reservoirs. J. Pet. Sci. Eng. 171, 1443–1454 (2018).

[14] Olabode, O. A. Effect of water and gas injection schemes on synthetic oil rim models. J. Pet. Explor. Prod. Technol. 10, 1343–1358 (2020).

[15] Wu, X. M., Hou, R. J., Zheng, Z. Y. et al. Effect of bottom water on subsequent water flooding and gas drive in fractured-vuggy carbonate oil reservoir. Petrol. Geol. Recovery Eff. 23, 111–115 (2016).

[16] Kang. B., Xiong, W., Zhang, Z. H. et al. A preferred method of gas injection unit in the fractured-vuggy reservoir. Sci. Technol. Eng. 13, 7629–7633 (2013).

[17] Shi, Y. Z., Qiao, T. B., Wang, W. J. et al. Experiment on effect evaluation of nitrogen displacement of fractured-vuggy reservoir. Contemp. Chem. Ind. 49, 2194–2202 (2020).

[18] Hui, J., Liu, X. L. Wang, Y. et al. Study on the mechanism of gas injection and oil substitution in fracture-vuggy reservoirs in Tahe Oilfield. Drill. Prod. Technol. 36, 55–57 (2013).

[19] Allal, M. A., Brancolini, A., Smail, F. et al. Miscible water alternating gas injection WAG field scale application in Algeria: An effective way to improve oil recovery, rejuvenate mature field and develop opportunities to stream gas sales. Proc. ADIPEC Conf.; 10.2118/216168-MS (2023).

[20] Shedid, S. A., Almehaideb, R. A., Zekri, A. Y. et al. Microscopic rock characterization and influence of slug size on oil recovery by CO_2 miscible flooding in carbonate oil reservoir. Proc. SPE Int. Improved Oil Recovery Conf.; 10.2118/97635-MS (2005).

[21] Hou, R. J., Zhang, L., Li, H. B. et al. Influencing factors on EOR nitrogen flooding in fractured-vuggy carbonate reservoir. Petrol. Geol. Recovery Eff. 22, 64–68 (2015).

[22] Wang, Z. H., Xiao, Y., Guo, P. et al. Gas-water flowing characteristics under high temperature and high pressure in fractured cavity carbonate gas reservoir. Petrol. Reservoir Eval. Dev. 7, 47–52 (2017).

[23] Wang, L., Yang, S. L., Peng, X. et al. Visual experiments on the occurrence characteristics of multi-type reservoir water in fracture-cavity carbonate gas reservoir. Acta Pet Sin. 39, 686–696 (2018).

[24] Chen, X. J. Visualized gas drive EOR experiments in fractured-vuggy reservoirs after waterflooding in Tahe oilfield. Xinjiang Petrol. Geol. 39, 473–479 (2018).

[25] Su, W., Hou, R. J., Zhao, T. et al. Experimental investigation on continuous N_2 injection to improve light oil recovery in multi-wells fractured-cavity unit. Petroleum. 3, 367–376 (2017).

[26] Li, J., Peng, C. Z., Wang, L. et al. Experimental study on the simulation of water flooding mechanism in fracture-vuggy carbonate reservoirs. Nat. Gas Explor. Dev. 31, 41–84 (2008).

[27] Xiong, Y., Kang, B., Deng, X. L. et al. Physical simulation of the full diameter of different development methods of fracture-vuggy carbonate condensate gas reservoirs. Xinjiang Oil Gas 8, 58–61 (2012).

[28] Zheng, Z. Y., Zhang, T. Q., Hou, R. J. et al. Visible research on remaining oil after nitrogen flooding in fractured-cavity carbonate reservoir. Petrol. Geol. Recovery Eff. **23**, 93–97 (2016).